Am J Transl Res 2024;16(9):4422-4435
www.ajtr.org /ISSN:1943-8141/AJTR0155120

Original Article

A novel simple suture method for establishing an orthotopic pancreatic cancer mouse model: a comparative study with two conventional methods

Xiaotong Zhang[1*], Fan Li[1*], Hongbin Yang[1], Hailan Xu[2], Aihui Wang[3], Qichen Jia[3], Li Zhang[2], Lei Liu[1]

[1]Department of Immunology, Chengde Medical University, Chengde 067000, Hebei, P. R. China; [2]Department of Oncology, The Affiliated Hospital of Chengde Medical University, Chengde 067000, Hebei, P. R. China; [3]Department of Nuclear Medicine, The Affiliated Hospital of Chengde Medical University, Chengde 067000, Hebei, P. R. China. [*]Equal contributors.

Received December 26, 2023; Accepted August 12, 2024; Epub September 15, 2024; Published September 30, 2024

Abstract: Objective: This study aims to evaluate the efficacy of a novel simple suture method in establishing an optimal animal model for preclinical research in pancreatic cancer. Methods: To establish a novel simple suture method, the tumor fragment was placed on the tail of the pancreas and securely wrapped into the pancreas, and compared with two conventional methods: the cell injection method and the tumor fragment embedding method. Subsequently, emission tomography/computed tomography scanning, gross anatomy observation, hematoxylin and eosin staining, and immunohistochemistry staining were performed to assess the effectiveness of these methods. Results: The emission tomography/computed tomography scanning and anatomical examinations confirmed the successful construction of orthotopic pancreatic cancer models using all three methods. Histopathological analysis of the orthotopic masses and metastatic lesions revealed malignant transformation with tumor infiltration into normal tissue. Comparative analysis demonstrated that the cell injection method was easy to perform but resulted in poor uniformity of tumor size and had high costs. The tumor fragment embedding method exhibited excellent uniformity of tumor size, with the highest tumor growth rates and a greater pancreatic impairment. In contrast, the novel simple suture method featured a relatively simple surgical procedure, slower growth rates, good uniformity of tumor size, and minimal pancreatic impairment. Conclusion: The novel simple suture method is the optimal protocol for establishing an orthotopic pancreatic cancer mouse model, providing a robust foundation for preclinical studies on pancreatic cancer.

Keywords: Pancreatic cancer, orthotopic, mouse model, PET/CT, C57BL/6N

Introduction

Pancreatic cancer is recognized as one of the most aggressive and lethal malignancies worldwide, and it may rank as the second leading cause of cancer-related deaths by 2030 [1]. The nonspecific symptoms of pancreatic cancer often lead to diagnosis at an advanced stage for the majority of patients [2]. Surgical resection remains the main treatment for pancreatic cancer. Despite efforts, alternative therapies such as radiation therapy, chemotherapy, and locoregional therapy have demonstrated limited success [3-6]. Numerous preclinical and clinical trials are currently underway to enhance the treatment effectiveness and prognosis of pancreatic cancer through immunotherapy. Various immunotherapeutic approaches, such as immune checkpoint inhibitors, cancer vaccines, adoptive cell therapy, and combination immunotherapy with other medications [7, 8], have shown promising results in treating patients with different types of cancer [9, 10]. Nonetheless, pancreatic cancer immunotherapy encounters significant challenges. Factors contributing to these challenges include the high tumor burden resulting in immunosuppression [11], the presence of non-immunogenic phenotypes in nearly all pancreatic cancers [12], and the dense fibrotic stroma or desmoplasia characterized by the excessive production of extracellular matrix and stromal cell pro-

https://doi.org/10.62347/JUDX2512

liferation [13]. Therefore, conducting an extensive analysis to characterize the immune microenvironment of pancreatic cancer is crucial for enhancing the effectiveness of immunotherapy in pancreatic cancer. Achieving this goal necessitates the use of animal models that accurately mimic the in vivo tumor microenvironments of patients.

In vivo models commonly utilize murine models and are categorized into three subgroups: spontaneous, genetically engineered, and implantation models. The spontaneous mouse model of pancreatic cancer is induced by direct or indirect exposure of the pancreas to carcinogenic factors. This model is often employed to study the progression of pancreatic intraepithelial neoplasia and ductal adenocarcinoma. However, limitations such as a lengthy induction period, high mortality rates, low tumor formation rates, and the development of other types of tumors restrict the widespread application of this spontaneous mouse model. Genetically engineered mice, on the other hand, are valuable for examining gene functions in vivo, investigating new treatment approaches, and assessing cancer prevention strategies. Nevertheless, tumorigenesis in these genetically engineered mice is triggered by the specific activation or inactivation of embryonic pancreatic genes, which differs from the natural development of pancreatic cancer in humans. Currently, the most commonly utilized mouse model for studying pancreatic cancer is the pancreatic cancer implantation model, where pancreatic cancer cells or tissues are transplanted into mice. This model includes the subcutaneous pancreatic cancer model and the orthotopic pancreatic cancer model. The subcutaneous model fails to replicate the tissue heterogeneity and microenvironment of pancreatic cancer, thus limiting its capability to accurately predict drug response [14]. In contrast, the orthotopic pancreatic cancer model, characterized by tumor development and metastasis in the pancreas, is preferred for evaluating drug efficacy against tumors or metastases. Therefore, the development of a more appropriate orthotopic pancreatic cancer model is essential for advancing pancreatic cancer research.

In this study, the C57BL/6N mouse was selected as the model organism due to its suitability for immunological research. A novel simple suture method was utilized to establish an orthotopic pancreatic cancer mouse model. This novel approach was then compared with two conventional methods: cell injection and tumor fragment embedding. The novel simple suture method may facilitate preclinical research in pancreatic cancer immunotherapy.

Materials and methods

Experimental animals and grouping

Sixty-four SPF-grade C57BL/6N mice, aged 6-8 weeks, comprising an equal number of males and females, were purchased from Beijing Weitong Lihua Experimental Animal Technology Co., Ltd. in Beijing, China. The mice were housed under controlled conditions of 21-25°C and 50-60% humidity, with ad libitum access to a standard diet and water. Ethics approval for this study was obtained from the Institutional Animal Ethics Committee of Chengde Medical University (Approval No: CDMULAC-20230920-024).

A subcutaneous pancreatic cancer model was established in five mice, while an additional three mice were employed to assess tumor fragment invasion through the pancreatic envelope in a novel simple suture model. The remaining 56 mice were randomized into four groups, with 14 mice in each group. The first group served as the control group, undergoing sham surgery with exposure of the pancreas but without the implantation of tumor cells or tissue. The other three groups underwent treatment using the cell injection method, the tumor fragment embedding method, and the novel simple suture method, respectively. Each procedure was carried out independently by two investigators. All surgeries were conducted under anesthesia using 0.4% pentobarbital sodium (40 mg/kg) administered intraperitoneally.

Cell culture

The murine pancreatic cancer cell line Pan02 was obtained from Shanghai Zhongqiao Xinzhou Biotechnology Co., Ltd. (Shanghai, China). The cells were cultured in DMEM (Gibco, USA) supplemented with 10% fetal bovine serum (Procell Life Science & Technology Co., Ltd., Beijing, China), penicillin (100 IU/mL)/strepto-

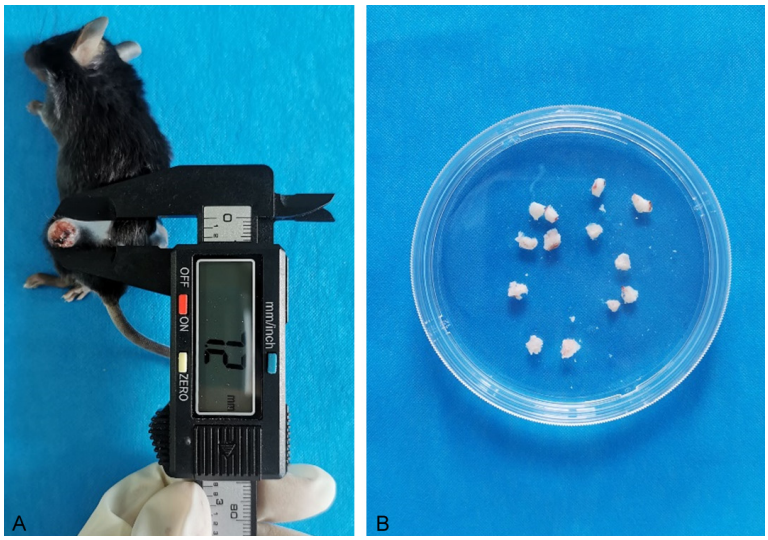

Figure 1. Preparation of tumor fragment from subcutaneous pancreatic cancer model. A. Subcutaneous pancreatic cancer model. B. The stripped tumor mass from the next-generation subcutaneous model.

mycin (100 μg/mL) at 37°C in a 5% CO_2 incubator. The medium was refreshed every 1-2 days, and cells were maintained until reaching 90% confluence before being subcultured or harvested for cryopreservation.

Subcutaneous pancreatic cancer model

Pan02 cells in the logarithmic growth phase were resuspended to a concentration of 1 × 10^6 cells/ml. Then, 200 μL of cell suspension was injected subcutaneously into the left flank of one C57BL/6N mouse to establish the first-generation subcutaneous pancreatic cancer model. Tumor formation was monitored every other day, and the tumor volumes were calculated using the formula of volume = $(width)^2$ × length/2. When the tumor volume reached 1 cm^3, the mice were humanely euthanized through cervical dislocation following an intraperitoneal injection of 0.4% pentobarbital sodium (40 mg/kg). The tumor tissues were excised, and cut into 1 mm^3 pieces, and four pieces of tumor tissue were transplanted subcutaneously into the left flank of four additional C57BL/6N mice to establish the next-generation subcutaneous pancreatic cancer models (**Figure 1A**). When the tumor volume reached 1 cm^3, the tumor masses from the four next-generation subcutaneous pancreatic cancer mice were excised, after which the capsule, blood vessels, and necrotic tissues were carefully dissected. The well-growing tumor tissues, resembling firm fish flesh, were then sectioned into 2 mm^3 pieces with a puncture needle and pooled for use in experiments involving the tumor fragment embedding method and the novel simple suture method (**Figure 1B**). The entire process, from tumor isolation to transplantation into mice, was completed within a strict time frame of 3 h.

Establishment of an orthotopic pancreatic cancer model using the cell injection method

Pan02 cells in the logarithmic growth phase were resuspended at a concentration of 2 × 10^7 cells/mL. The cell suspension was then mixed with Matrigel matrix (BD Biosciences, San Diego, CA) at a ratio of 1:1. Anesthesia was induced in C57BL/6N mice, followed by making an abdominal incision to expose the spleen and locate the pancreas. Using a sterile syringe, 0.1 mL of the mixture (1 × 10^6 Pan02 cells) was injected into the subcapsule of the pancreatic tail. The cell suspension was well mixed before each sample aspiration. The needle was retained in the pancreas for 10 seconds post-injection to prevent fluid leakage before being slowly withdrawn. Pressure was applied with a cotton ball, and the muscle layer and skin incisions were closed using a sterile 7-0 absorbable suture (**Figure 2A**).

Establishment of an orthotopic pancreatic cancer model using the tumor fragment embedding method

After anesthesia, a 0.5 cm incision was surgically made in the lower left abdomen to expose the spleen and pancreas. Subsequently, a 3 mm incision was carefully made in the pancreas's tail using ophthalmic scissors. A tumor fragment of 2 mm^3 was then selected at random from the pooled tumor pieces and implanted into the pancreas. Finally, the muscle layer and skin incision were closed with a sterile 7-0 absorbable suture (**Figure 2B**).

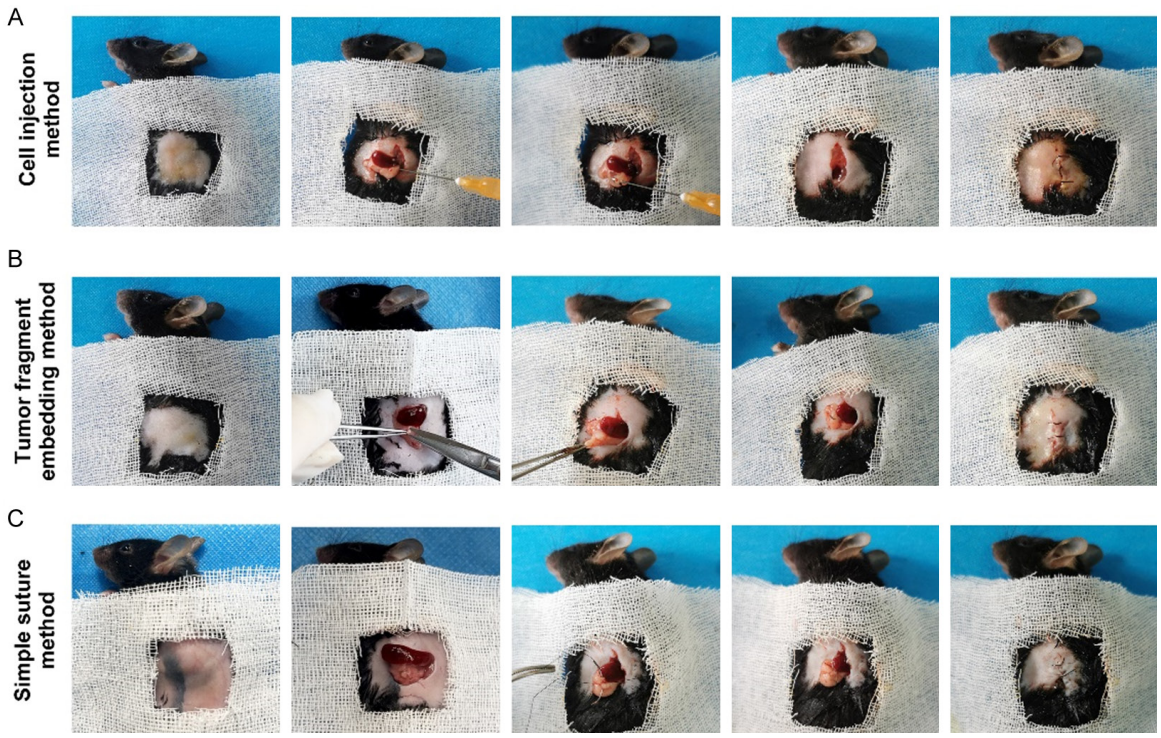

Figure 2. Surgical procedure of three orthotopic pancreatic cancer mouse models. A. Cell injection method. B. Tumor fragment embedding method. C. Novel simple suture method.

Establishment of an orthotopic pancreatic cancer model using the novel simple suture method

After anesthesia, the spleen and pancreas were exposed. A tumor fragment of 2 mm^3 was randomly selected from pooled tumor pieces and placed on the tail of the pancreas. The suture was carefully passed through the upper and lower parts of the pancreatic tissue using a sterile 8-0 absorbable suture and gradually tightened to secure and wrap the tumor fragment within the pancreas. Subsequently, the muscle layer and skin incision were closed in sequence (**Figure 2C** and Supplementary Video 1).

Positron emission tomography/computed tomography (PET/CT)

On the 14th day post-modeling, PET/CT scanning was conducted on four groups of mice, with the control group mice serving as the norm for metabolic profiles. The mice were subjected to a 6-h fasting period and water deprivation before the examination. Then, the mice received intravenous administration of 100 μCi of 18F-FDG through the tail vein. After 50 min, anesthesia was induced by intraperitoneal injection of 0.4% pentobarbital sodium, and the PET/CT scans were carried out utilizing a Siemens Biograph 64 PET/CT scanner (Siemens, Erlangen, Germany). The information such as mouse identification number, scanning date, and administered radiotracer activity was entered into the system. The helical CT scan was conducted utilizing the following parameters: tube voltage of 120 kV, tube current of 300 mA, slice thickness of 3.75 mm, interslice spacing of 2.5 mm, pitch of 0.531:1, and a field of view of 20 cm. Subsequent PET scans were conducted in three-dimensional mode, covering 2-bed positions with each having an acquisition time of 4 min. Image fusion and analysis were carried out using DICOM Viewer software version 3.4.1 (Syno Union Medical Technology Co., Ltd., Beijing, China). A three-dimensional region of interest was delineated on the PET/CT fused image of each mouse to quantify 18F-FDG uptake. The maximum standard uptake value (SUVmax) was calculated using the formula: SUVmax = maximum activity in a region of interest (MBq/g)/[injected dose (MBq)/body weight (g)].

Anatomical observation

On the 15th day after modeling, the mice were humanely euthanized through cervical dislocation following an intraperitoneal injection of 0.4% pentobarbital sodium (40 mg/kg). The solid tumors in the pancreas were dissected and weighed. The long diameter (L) and short diameter (W) of tumors were measured with a caliper and the tumor volume was calculated by the formula of $V = (L \times W^2)/2$. Additionally, metastatic lesions in organs such as the liver, spleen, lung, and intestine were observed, dissected, and assessed for tumor formation, growth rate, organ metastasis, and the presence of ascites.

Histopathological examination

Pancreatic cancer tissue and major organs including the lungs, liver, spleen, intestine, and kidneys were extracted and fixed in 4% paraformaldehyde, embedded in paraffin, and sectioned at 5 μm thickness, followed by routine hematoxylin and eosin staining. Cell morphology was observed under light microscopy. For immunohistochemistry, the paraffin sections were deparaffinized, followed by antigen repair and blocking with bovine serum albumin. Incubation with the primary antibody of rabbit polyclonal anti-Ki67 (1:50; Wanleibio, Beijing, China) was performed overnight at 4°C. Subsequently, the sections were incubated with horseradish peroxidase-labeled goat anti-rabbit/mouse IgG antibody. Diaminobenzidine was used for color development. After counterstaining with hematoxylin for 1 min, 1% hydrochloric acid alcohol differentiation for 3 sec, dehydration, and transparency, the sections were observed under a light microscope. The optical density was quantified using ImageJ software (Maryland, USA).

Statistical analysis

Statistical analysis was conducted using SPSS 22.0 (SPSS Inc., Chicago, IL, USA). Tumor weight, volume, and mean growth rate are presented as means ± standard deviation. One-way analysis of variance (ANOVA) with Fisher's least significant difference (LSD) test was used for comparing multiple groups, with statistical significance set at $P<0.05$.

Results

The radiotracer uptake is higher in the three orthotopic pancreatic cancer mouse model groups

On the 14th day after modeling, the mice underwent PET/CT scanning and subsequent three-dimensional reconstruction (Supplementary Figure 1). The PET/CT fusion images (**Figure 3A**) revealed increased radiotracer uptake in various regions, including the brain, back fat pad, heart, bladder, and occasionally in the upper limb and calf muscles among all groups of mice. In contrast, the control group mice displayed typical radiotracer distribution in baseline conditions. Furthermore, examination of transverse, sagittal, and coronal plane images unveiled significantly higher radiotracer uptake in the peritoneal cavities of mice in the cell injection group, tumor fragment embedding group, and novel simple suture group. Additionally, the novel simple suture method group showed mild high radiotracer uptake in multiple regions of the peritoneal cavity, indicating potential metastasis in the peritoneal cavity. The SUVmax for the control, cell injection method, tumor fragment embedding method, and novel simple suture method groups were 19.530±1.630 g/ml, 60.520±7.830 g/ml, 120.820±15.480 g/ml, and 49.320±1.050 g/ml, respectively (**Figure 3B**). Significant differences were observed compared to the control group in the cell injection method group ($P=0.007$), the tumor fragment embedding method group ($P<0.001$), and the novel simple suture method group ($P=0.037$). Furthermore, the SUVmax in the cell injection method group ($P<0.001$) and the novel simple suture method group ($P<0.001$) were significantly lower than that in the tumor fragment embedding method group, suggesting a slower growth rate in the novel simple suture method group compared to the tumor fragment embedding method group (**Table 1**).

The novel simple suture method group has the slowest tumor growth rate and consistent tumor size

On the 15th day after modeling, the tumor growth and metastasis were observed. On the 15th day post-modeling, the mice were anesthetized and dissected to observe tumor growth

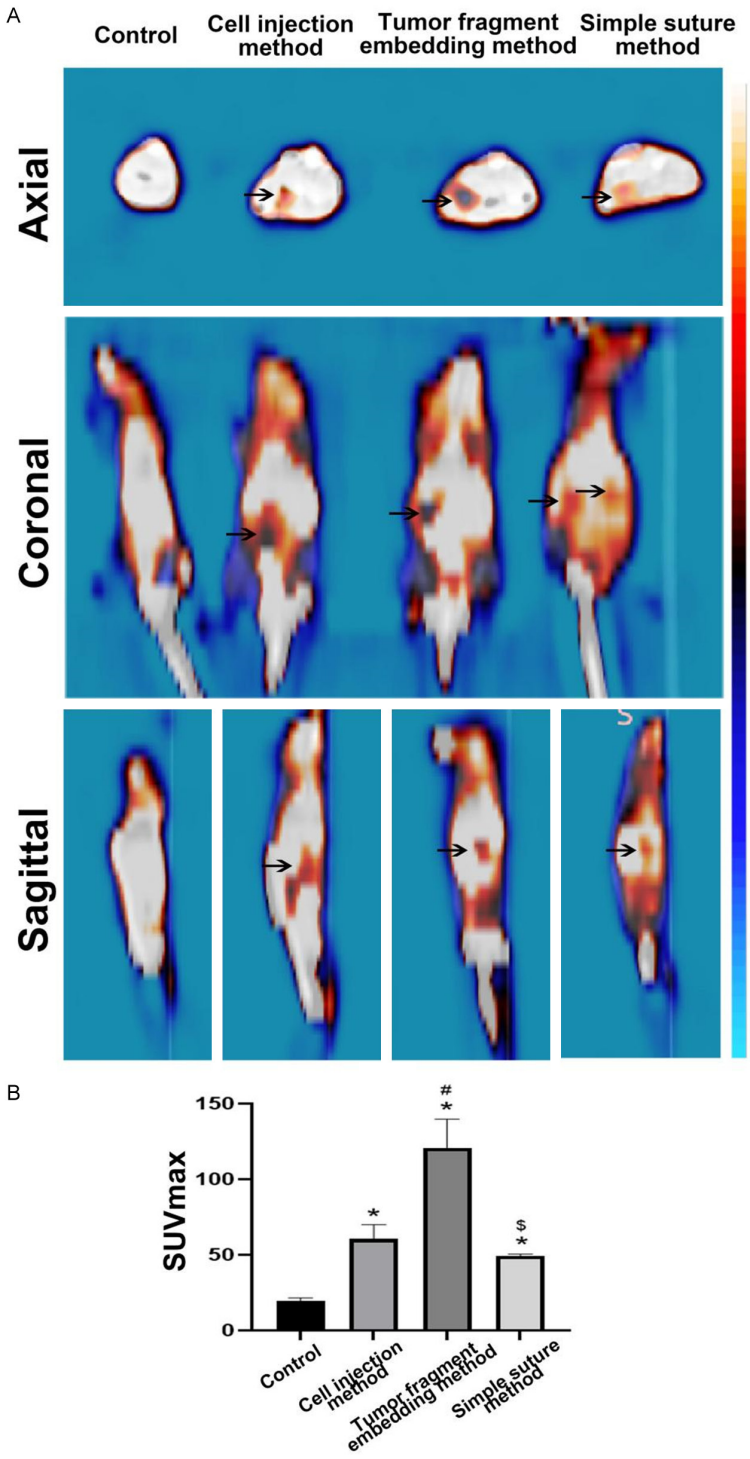

Figure 3. PET/CT images. A. Transverse, sagittal, and coronal plane images. B. SUVmax value of three orthotopic mouse model groups. *P<0.05 vs. Control group; #P<0.05 vs. Cell injection method group. $$P$<0.05 vs. Tumor fragment embedding method group.

and metastasis. The findings revealed that pancreatic tumors were present in all 42 mice, with a tumor formation rate of 100% in the cell injection method group (14/14), the tumor fragment embedding method group (14/14), and the novel simple suture method group (14/14) (**Figure 4A**). Subsequently, the implanted tumors from each group were excised, photographed, and weighed (**Figure 4B**). The average weight of orthotopic tumors in the tumor fragment embedding method group was 0.348±0.079 g, significantly higher than that in the cell injection method group 0.221±0.119 g (P=0.001) and the novel simple suture method group 0.213±0.065 g (P=0.002) (**Figure 4C** and **Table 1**). Moreover, the mean tumor growth rates varied among different groups: the fastest growth rate was observed in the tumor fragment embedding method group 24.393±4.762 mm^3/day, followed by the cell injection method group 17.658±8.108 mm^3/day, with the slowest growth rate recorded in the novel simple suture method group 17.220±3.318 mm^3/day (**Table 1**). Additionally, the standard deviations of tumor weight, tumor volumes, and tumor growth rate were significantly different in the cell injection, tumor fragment embedding, and novel simple suture method groups (**Figure 4D**). This suggests a wider range of tumor sizes in the cell injection group, while the tumor sizes were more consistent in the tumor fragment embedding and novel simple suture method groups.

Additionally, we found that the spleen was the most common site of metastasis in the orthotopic pancreatic cancer mouse model. Specifically, spleen meta-

Table 1. Comparison of the novel simple suture method with the cell injection and tumor fragment embedding methods

Model	Tumor formation	SUVmax (g/ml)	Mean tumor weight (g)	Mean tumor volume (mm^3)	Implantation days (d)	Mean growth rate (mm^3/d)	Spleen metastasis	Intestine metastasis	Presence of ascites	HE staining	Relative Ki67 expression	Surgery Time (sec)	Pancreatic Injury
Cell injection method	14/14	60.520± 7.830	0.221± 0.119	264.883± 121.616	15	17.658± 8.108	6/14	4/14	2/14	Significant Nuclear Atypia	0.359± 0.175	248±36	Edema
Tumor fragment embedding method	14/14	120.820± 15.480*	0.348± 0.079*	365.900± 71.431*	15	24.393± 4.762*	8/14	7/14	3/14	Significant Nuclear Atypia	0.365± 0.110	486±48	Oozing of blood
Simple suture method	14/14	49.320± 1.050#	0.213± 0.065#	258.302± 49.764#	15	17.220± 3.318#	9/14	9/14	5/14	Significant Nuclear Atypia	0.359± 0.120	356±53	Petechiae

*P<0.05 vs. Cell injection method group; #P<0.05 vs. Tumor fragment embedding method group.

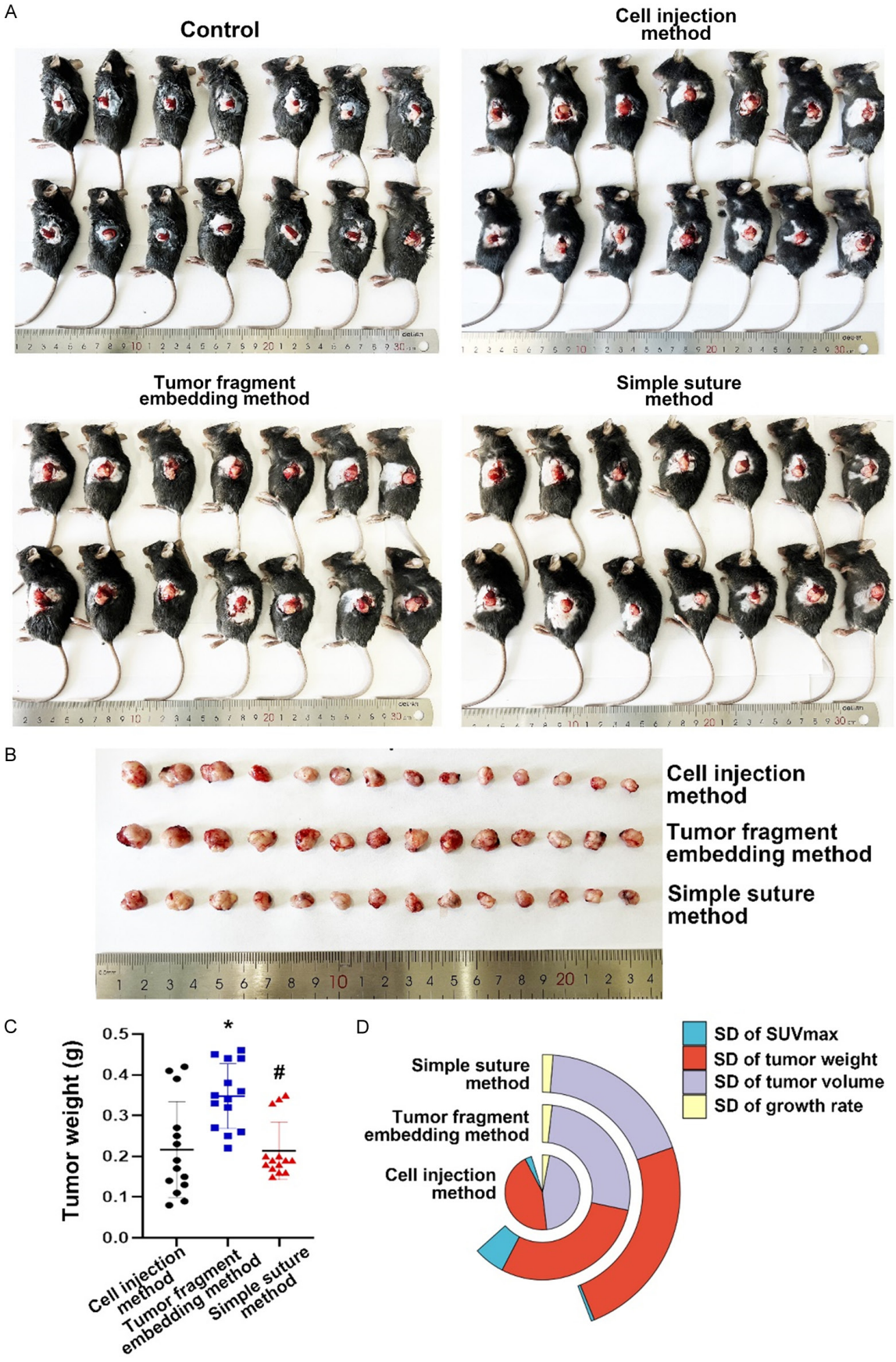
A
Control
Cell injection method
Tumor fragment embedding method
Simple suture method
B
Cell injection method
Tumor fragment embedding method
Simple suture method
C
Tumor weight (g)
0.5
0.4
0.3
0.2
0.1
0.0
*
#
Cell injection method
Tumor fragment embedding method
Simple suture method
D
Simple suture method
Tumor fragment embedding method
Cell injection method
SD of SUVmax
SD of tumor weight
SD of tumor volume
SD of growth rate

Figure 4. Anatomical observation. A. Formation of orthotopic pancreatic tumors in four groups. B. The removed pancreatic tumors. C. The tumor weight. $^{*}P<0.05$ vs. Cell injection method group. $^{\#}P<0.05$ vs. Tumor fragment embedding method group. D. Standard deviations of SUVmax, tumor weight, tumor volume, and tumor growth rate in the three method groups. Ring proportion represents the differences within groups.

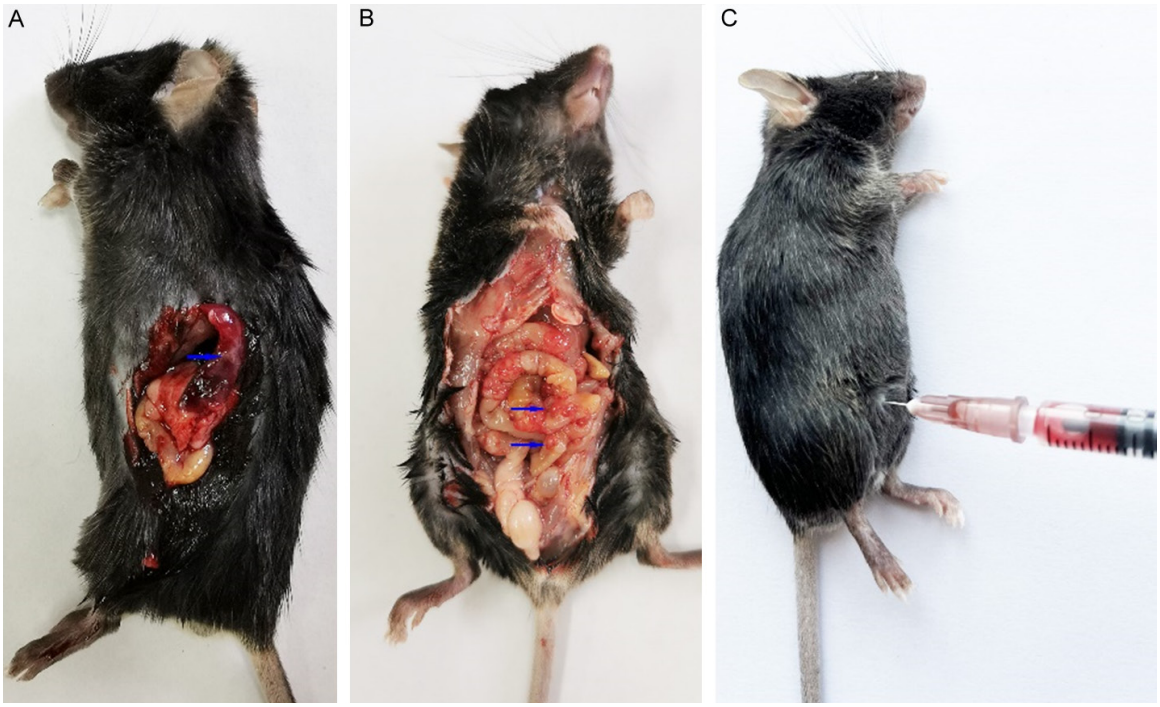

Figure 5. Gross observation of organ metastasis. A. Spleen metastasis. B. Intestine metastasis. C. Ascites formation.

stases were observed in 6 mice in the cell injection group, 8 mice in the tumor fragment embedding group, and 9 mice in the novel simple suture group (**Figure 5A** and **Table 1**). Intestinal metastases were identified in 4 mice in the cell injection group, 7 mice in the tumor fragment embedding group, and 9 mice in the novel simple suture group (**Figure 5B** and **Table 1**). Given that intestinal metastasis is associated with an increased risk of ascite formation, ascites were present in 2 mice in the cell injection group, 3 mice in the tumor fragment embedding group, and 5 mice in the novel simple suture group (**Figure 5C** and **Table 1**). Notably, no metastases were detected in the liver, lungs, or kidneys.

Cellular atypia and invasiveness in the three orthotopic pancreatic cancer mouse model groups

Hematoxylin and eosin staining revealed no histopathological differences among the three orthotopic pancreatic cancer mouse model groups. The tumors displayed characteristics of poorly differentiated tumor cells, exhibiting irregularly shaped nuclei with dark staining and a lack of polarity, along with lobulated nucleoli (**Figure 6A**). Moreover, the tumors displayed high invasiveness, infiltrating the adjacent normal tissue. Furthermore, Hematoxylin and eosin staining was also performed in major organs including the lungs, liver, spleen, intestine, and kidneys, and the results showed significant evidence in the metastatic spleen and intestine tissues (**Figure 6B**).

The invasion of tumor fragments through the pancreatic envelope was observed in three additional mice following orthotopic implantation of pancreatic cancer using the novel simple suture method. On the 6th day post-operation, the mice were euthanized, and their pancreas was examined using hematoxylin and eosin staining. The findings revealed hyperchromatic cells with large nuclei in the sutured tumor tissue, indicative of cancerous properties. The boundaries between the tumor tissue

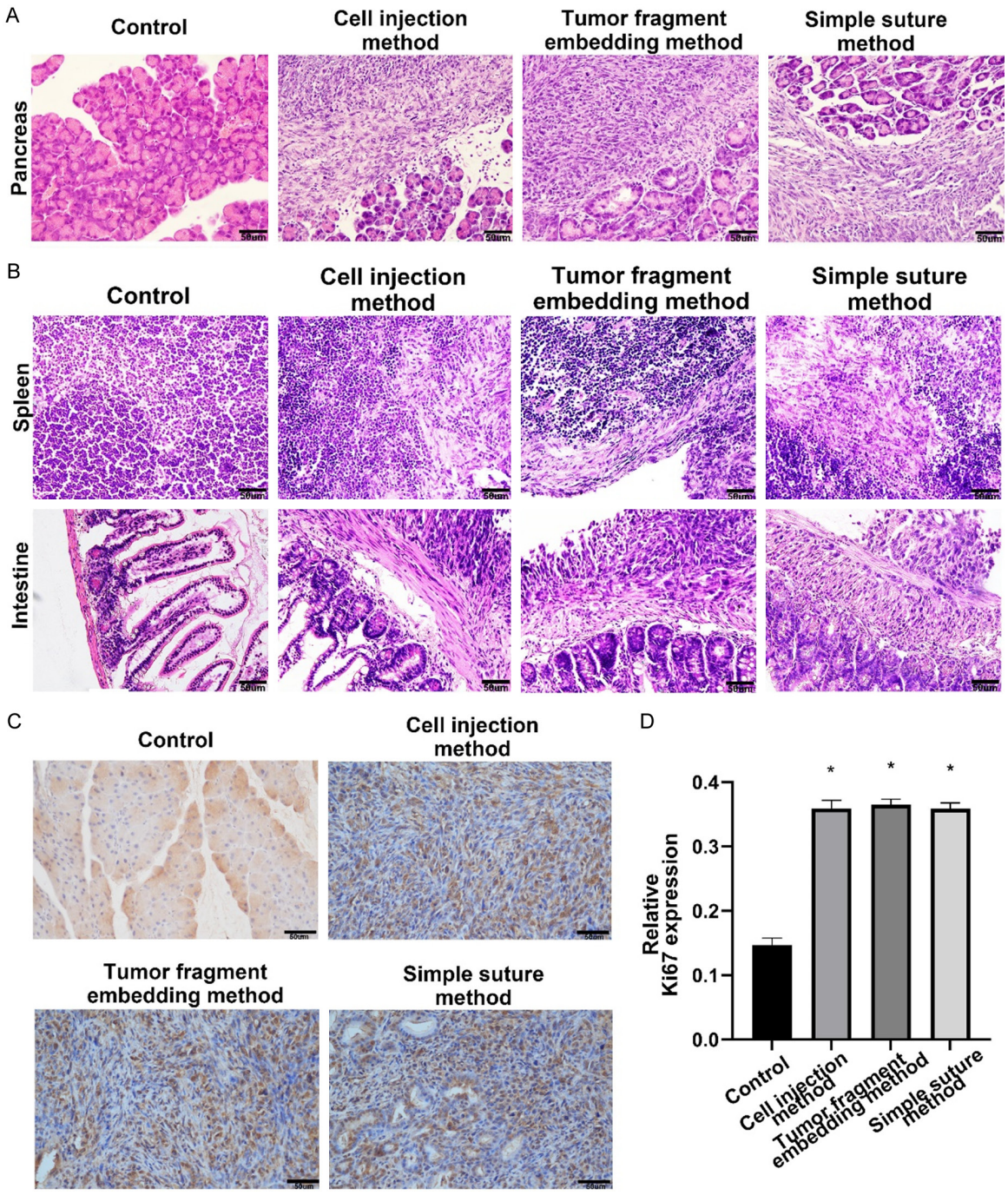

Figure 6. Histopathological observation. A. Hematoxylin and eosin staining in orthotopic pancreatic cancer (×400 magnification). Scale bars 50 uM. B. Hematoxylin and eosin staining in the metastatic spleen and intestine tissue (×400 magnification). Scale bars 50 uM. C. Ki67 immunohistochemistry staining in orthotopic pancreatic cancer (×400 magnification). Scale bars 50 uM. D. Quantification of Ki67 staining. $^{*}P<0.05$ vs. Control group.

and the normal pancreatic tissue were generally unclear, accompanied by disruption and destruction of the pancreatic envelope. The tumor cells infiltrated the adjacent normal pancreatic tissues, leading to pronounced malignant alterations in the pancreatic cells at the boundaries, characterized by significant atypia, mitotic activity, and hyperchromatic nuclei (**Figure 7**). Capsular invasion in pancreatic cancer is likely to involve multiple mechanisms,

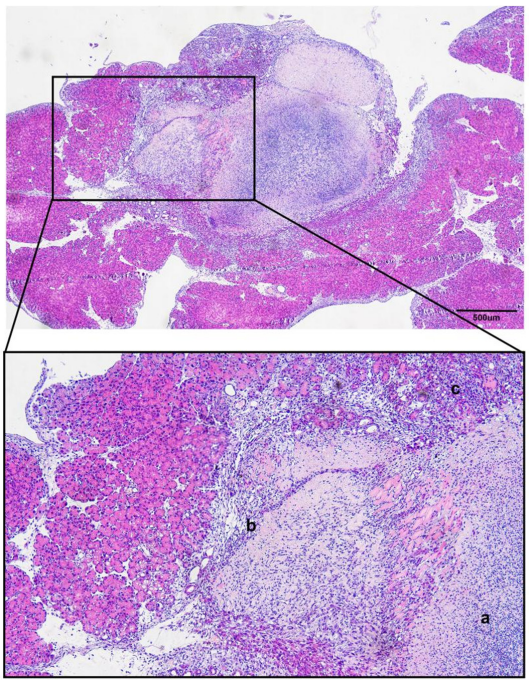

Figure 7. Hematoxylin and eosin staining in the invasion of tumor fragments through the pancreatic envelope using the novel simple suture method (×40 magnification). Scale bars 500 uM. A. Tumor fragment. B. Invaded pancreatic envelope. C. Invaded pancreatic tissue.

including invasion of the tumor cells in the pancreatic envelope through tiny pores or fissures, the release of proteases to degrade the envelope tissue protein, and loss of the normal barrier function of the pancreatic envelope due to changes in the tumor microenvironment.

Immunohistochemistry revealed a positive expression of Ki67 in the three orthotopic pancreatic cancer mouse model groups (**Figure 6C**). Compared with the control group, there were significant differences in the cell injection method group ($P<0.001$), the tumor fragment embedding method group ($P<0.001$), and the simple suture method group ($P<0.001$), indicating an activation of pancreatic cancer cell proliferation in these groups (**Figure 6D**).

Discussion

The two most common mouse models used for studying pancreatic cancer are subcutaneous and orthotopic models. In subcutaneous models, the tumor grows superficially, allowing for easy access, direct observation, and precise measurement, which facilitates monitoring of tumor progression. In a study by Conti et al. [15], 4 × 10^6 PaCa44 pancreatic cancer cells were subcutaneously injected into the right flank of CD1 nude mice to establish a subcutaneous xenograft model of pancreatic cancer. Tumor volume was monitored using a vernier caliper to assess tumor growth and evaluate the treatment efficacy of HFt-MP-PASE-MIT nanoformulation. However, the subcutaneous model lacks the tendency for distant metastases and does not fully replicate the tumor microenvironment of human pancreatic cancer. The orthotopic model is considered more suitable for mimicking the local tumor microenvironment and distant metastases, and accurately predicting the efficacy of drug treatments in vivo. Zhao et al. [16] demonstrated that a combination of irreversible electroporation and programmed cell death protein 1 blockade could enhance the infiltration of intratumoral $CD8^+$ lymphocytes and substantially extend survival in a murine orthotopic pancreatic cancer model, inducing a durable memory immune response. This study focused on establishing an orthotopic pancreatic cancer mouse model to provide a robust foundation for investigating the tumor microenvironment and immunotherapy in pancreatic cancer.

Commonly used mice in constructing tumor models include BALB/c, C57BL/6, nude, SCID, NSG, etc. Among these, C57BL/6, an inbred strain, stands out for its immunogenicity and is frequently used in immunological and antitumor activity studies [17]. Chen et al. [18] inoculated Panc02 cells subcutaneously into the right and left flank of C57BL/6 mice to establish primary and metastatic tumors. They demonstrated that a combination treatment involving Titanium diselenide-mediated sonodynamic therapy and programmed cell death protein 1 blockade effectively activated anti-tumor immune responses through the induction of immunogenic cell death, leading to the suppression of tumor growth and metastasis. There are two major lineages of C57BL/6 mice: C57BL/6J and C57BL/6N. In C57BL/6J mice, chemokine levels are reduced due to a mutation in the Nlrp12 gene, affecting immune infiltration and pathogen clearance [19]. In this study, C57BL/6N mice lacking the Nlrp12 mutation were selected to establish an orthotopic pancreatic cancer model, aiming to closely mimic the human disease condition and pro-

vide a more robust animal model for further experimental investigations.

The construction of the orthotopic pancreatic cancer model currently presents multiple challenges, including complex procedures, high costs, and the risk of severe pancreatic damage. Various strategies, such as the cell injection method and the tumor fragment embedding method, have been explored by researchers to address these issues. The cell injection method involves the direct injection of pancreatic cancer cells into the mouse pancreas. In a pioneering study dating back to 1985, Tan et al. [20] successfully established an orthotopic xenograft model of human pancreatic tumors by inoculating AsPC-1 cells into the duodenal lobe of the pancreas in athymic nude mice. In our model construction using the cell injection method, Pan02 cells from mouse pancreatic tumors were combined with the Matrigel matrix. Once the mixture reached room temperature, it would solidify into a gel-like substance. Subsequently, upon introduction of the cell suspension into the mouse pancreas, the gel-like substance formed a barrier at the injection site, effectively preventing any potential cell overflow. While this approach successfully mitigated issues related to pressure build-up and minimized the risk of uneven cell distribution inherent in manual procedures, it was not without limitations. Variability in tumor sizes within the model system suggested a lack of uniformity. Furthermore, the substantial cell quantities, extensive culture times, and high costs associated with meeting the demand for modeled mice underscore significant limitations of the cell injection method.

Another traditional model construction method is the tumor fragment embedding method. Hwang et al. [21] subcutaneously injected murine pancreatic cancer Pan02 cells into the flanks of nude mice. A tumor fragment of 3 mm^3 obtained from a subcutaneous tumor was then orthotopically transplanted into the pancreatic tail of C57BL/6 mice, either with or without splenectomy. The same method was also used in this study. Initially, the subcutaneous tumor was excised and cut into fragments of 2 mm^3. Subsequently, a 3 mm incision was made in the pancreas tail. A tumor fragment was then embedded into the incision. Finally, the incision was sutured. We observed that the tumor morphology remained intact, exhibiting enhanced uniformity. This method obviates the need for supplementary cell culture as it involves direct implantation of well-developed subcutaneous tumor fragments, thus resulting in substantial time and cost savings. Nonetheless, the rapid tumor growth associated with the fragment embedding method hinders the effective monitoring of antitumor treatment efficacy over extended therapy periods. Furthermore, the surgical procedure is intricate and time-intensive, posing a notable challenge. Of particular concern is the inadvertent dissection of the pancreas during surgery, leading to significant pancreatic injury (**Table 1**).

In this study, we developed a novel and simple suture method for establishing an orthotopic pancreatic cancer mouse model. A key step of this method involved securely wrapping the tumor fragment within the pancreas to prevent the tumor tissue from dislodging into the peritoneal cavity. This novel method achieved a remarkable 100% success rate in implantation and minimized pancreatic damage by eliminating the need for pancreas incision. Additionally, it offered several advantages, such as a slower growth rate, simple operation, and less time-consuming (**Table 1**). However, the failure to encapsulate the tumor beneath the capsule in this model increases its susceptibility to abdominal metastasis.

An orthotopic pancreatic tumor in the intra-abdominal cavity poses challenges in monitoring its growth unlike a subcutaneous tumor model, thus necessitating imaging examinations. Commonly employed detection techniques for intra-abdominal tumors include in vivo imaging of small animals [22], laparoscopes, nuclear magnetic resonance [23], and CT scans. PET/CT, an emerging diagnostic technology extensively utilized in the clinical diagnosis of various tumors [24, 25], offers significant advantages. By integrating PET data on metabolic changes with detailed anatomic CT information, PET/CT enables early lesion detection and provides more precise location information compared to CT or PET alone [26]. Moreover, PET/CT plays a crucial role in monitoring the in vivo tumor growth of small animals. Wang et al. [27] utilized 18F-FDG PET/CT imaging to assess the treatment response in an orthotopic xenograft nude-mouse model established using the

human SGC-7901 gastric cancer cell line. They demonstrated that glycolysis and tumor growth were suppressed by intraperitoneal injection of 3-bromopyruvate and sodium citrate. In our study, PET/CT was used to monitor in vivo tumor growth in the mouse model. The region of interest was delineated on the fused PET/CT images to calculate the SUVmax in each mouse. SUVmax is a common metric for evaluating tumor metabolic activity and biological characteristics. A high SUVmax often indicates that tumor cells are in a metabolically active state, associated with aggressive and metastatic malignant phenotypes [28]. In preclinical experiments, PET/CT imaging is used to observe in vivo tumor growth in animal models, with the SUVmax value reflecting the treatment response. This non-invasive approach provides valuable insights for further research on the clinical management of pancreatic cancer.

Conclusion

In this study, three methods were employed to construct orthotopic pancreatic cancer mouse models. Their strengths and weaknesses were compared. The cell injection method, despite being relatively simple, was costly and lacked uniformity. In contrast, the tumor fragment embedding method group displayed better uniformity and aligned more closely with pancreatic cancer characteristics, yet induced significant damage to the pancreas. The novel simple suture method, on the other hand, offered a simpler procedure with minimal pancreatic damage and better uniformity of tumors. This method emerges as the ideal approach for constructing orthotopic pancreatic cancer mouse models. Pancreatic cancer is a highly lethal malignancy presenting a significant therapeutic challenge. Immunotherapy emerges as a novel and promising treatment approach. The establishment of an ideal animal model is crucial for accurately assessing the efficacy of immunotherapy, thereby offering critical support for clinical translation.

Acknowledgements

This study was supported by the National Natural Science Foundation of China (No. 81703001), the Natural Science Foundation of Hebei Province (Nos. H2021406021; H2024406046), Hebei Province Government-Funded Clinical Medical Outstanding Talents Project, Hebei Province Medical Science Research Project (Nos. 20210247; 20221335), and Chengde Medical University Scientific Research Major Projects (No. KY2020005).

Disclosure of conflict of interest

None.

Address correspondence to: Lei Liu, Department of Immunology, Chengde Medical University, Anyuan Road, Chengde 067000, Hebei, P. R. China. Tel: +86-0314-2517004; E-mail: homingreceptor@hotmail.com; liul@cdmc.edu.cn; Li Zhang, Department of Oncology, The Affiliated Hospital of Chengde Medical University, No. 34th Nanyingzi Street, Chengde 067000, Hebei, P. R. China. Tel: +86-0314-2279702; E-mail: cd_zhangl@126.com

References

[1] Rahib L, Smith BD, Aizenberg R, Rosenzweig AB, Fleshman JM and Matrisian LM. Projecting cancer incidence and deaths to 2030: the unexpected burden of thyroid, liver, and pancreas cancers in the United States. Cancer Res 2014; 74: 2913-2921.

[2] Raut CP, Tseng JF, Sun CC, Wang H, Wolff RA, Crane CH, Hwang R, Vauthey JN, Abdalla EK, Lee JE, Pisters PW and Evans DB. Impact of resection status on pattern of failure and survival after pancreaticoduodenectomy for pancreatic adenocarcinoma. Ann Surg 2007; 246: 52-60.

[3] Li HY, Cui ZM, Chen J, Guo XZ and Li YY. Pancreatic cancer: diagnosis and treatments. Tumour Biol 2015; 36: 1375-1384.

[4] Lin QJ, Yang F, Jin C and Fu DL. Current status and progress of pancreatic cancer in China. World J Gastroenterol 2015; 21: 7988-8003.

[5] Ercan G, Karlitepe A and Ozpolat B. Pancreatic cancer stem cells and therapeutic approaches. Anticancer Res 2017; 37: 2761-2775.

[6] Schizas D, Charalampakis N, Kole C, Economopoulou P, Koustas E, Gkotsis E, Ziogas D, Psyrri A and Karamouzis MV. Immunotherapy for pancreatic cancer: a 2020 update. Cancer Treat Rev 2020; 86: 102016.

[7] Igarashi Y and Sasada T. Cancer vaccines: toward the next breakthrough in cancer immunotherapy. J Immunol Res 2020; 2020: 5825401.

[8] Cha JH, Chan LC, Song MS and Hung MC. New approaches on cancer immunotherapy. Cold Spring Harb Perspect Med 2020; 10: a036863.

[9] Le DT, Durham JN, Smith KN, Wang H, Bartlett BR, Aulakh LK, Lu S, Kemberling H, Wilt C, Luber BS, Wong F, Azad NS, Rucki AA, Laheru D,

Donehower R, Zaheer A, Fisher GA, Crocenzi TS, Lee JJ, Greten TF, Duffy AG, Ciombor KK, Eyring AD, Lam BH, Joe A, Kang SP, Holdhoff M, Danilova L, Cope L, Meyer C, Zhou S, Goldberg RM, Armstrong DK, Bever KM, Fader AN, Taube J, Housseau F, Spetzler D, Xiao N, Pardoll DM, Papadopoulos N, Kinzler KW, Eshleman JR, Vogelstein B, Anders RA and Diaz LA Jr. Mismatch repair deficiency predicts response of solid tumors to PD-1 blockade. Science 2017; 357: 409-413.

[10] Sharma P, Callahan MK, Bono P, Kim J, Spiliopoulou P, Calvo E, Pillai RN, Ott PA, de Braud F, Morse M, Le DT, Jaeger D, Chan E, Harbison C, Lin CS, Tschaika M, Azrilevich A and Rosenberg JE. Nivolumab monotherapy in recurrent metastatic urothelial carcinoma (CheckMate 032): a multicentre, open-label, two-stage, multiarm, phase 1/2 trial. Lancet Oncol 2016; 17: 1590-1598.

[11] Feng M, Xiong G, Cao Z, Yang G, Zheng S, Song X, You L, Zheng L, Zhang T and Zhao Y. PD-1/PD-L1 and immunotherapy for pancreatic cancer. Cancer Lett 2017; 407: 57-65.

[12] Pico de Coaña Y, Choudhury A and Kiessling R. Checkpoint blockade for cancer therapy: revitalizing a suppressed immune system. Trends Mol Med 2015; 21: 482-491.

[13] Thomas D and Radhakrishnan P. Tumor-stromal crosstalk in pancreatic cancer and tissue fibrosis. Mol Cancer 2019; 18: 14.

[14] Ho WJ, Jaffee EM and Zheng L. The tumour microenvironment in pancreatic cancer - clinical challenges and opportunities. Nat Rev Clin Oncol 2020; 17: 527-540.

[15] Conti G, Pitea M, Ossanna R, Opri R, Tisci G, Falvo E, Innamorati G, Ghanem E, Sbarbati A, Ceci P and Fracasso G. Mitoxantrone-loaded nanoferritin slows tumor growth and improves the overall survival rate in a subcutaneous pancreatic cancer mouse model. Biomedicines 2021; 9: 1622.

[16] Zhao J, Wen X, Tian L, Li T, Xu C, Wen X, Melancon MP, Gupta S, Shen B, Peng W and Li C. Irreversible electroporation reverses resistance to immune checkpoint blockade in pancreatic cancer. Nat Commun 2019; 10: 899.

[17] Song HK and Hwang DY. Use of C57BL/6N mice on the variety of immunological researches. Lab Anim Res 2017; 33: 119-123.

[18] Chen L, Xue W, Cao J, Zhang S, Zeng Y, Ma L, Qian X, Wen Q, Hong Y, Shi Z and Xu Y. $TiSe_2$-mediated sonodynamic and checkpoint blockade combined immunotherapy in hypoxic pancreatic cancer. J Nanobiotechnology 2022; 20: 453.

[19] Ulland TK, Jain N, Hornick EE, Elliott EI, Clay GM, Sadler JJ, Mills KA, Janowski AM, Volk AP, Wang K, Legge KL, Gakhar L, Bourdi M, Ferguson PJ, Wilson ME, Cassel SL and Sutterwala FS. Nlrp12 mutation causes C57BL/6J strain-specific defect in neutrophil recruitment. Nat Commun 2016; 7: 13180.

[20] Tan MH and Chu TM. Characterization of the tumorigenic and metastatic properties of a human pancreatic tumor cell line (AsPC-1) implanted orthotopically into nude mice. Tumour Biol 1985; 6: 89-98.

[21] Hwang HK, Murakami T, Kiyuna T, Kim SH, Lee SH, Kang CM, Hoffman RM and Bouvet M. Splenectomy is associated with an aggressive tumor growth pattern and altered host immunity in an orthotopic syngeneic murine pancreatic cancer model. Oncotarget 2017; 8: 88827-88834.

[22] Kunnumakkara AB, Sung B, Ravindran J, Diagaradjane P, Deorukhkar A, Dey S, Koca C, Tong Z, Gelovani JG, Guha S, Krishnan S and Aggarwal BB. Zyflamend suppresses growth and sensitizes human pancreatic tumors to gemcitabine in an orthotopic mouse model through modulation of multiple targets. Int J Cancer 2012; 131: E292-E303.

[23] Tyagi P, Moon CH, Connell M, Ganguly A, Cho KJ, Tarin T, Dhir R, Sholosh B and Maranchie J. Intravesical contrast-enhanced MRI: a potential tool for bladder cancer surveillance and staging. Curr Oncol 2023; 30: 4632-4647.

[24] Li R, Ravizzini GC, Gorin MA, Maurer T, Eiber M, Cooperberg MR, Alemozzaffar M, Tollefson MK, Delacroix SE and Chapin BF. The use of PET/CT in prostate cancer. Prostate Cancer Prostatic Dis 2018; 21: 4-21.

[25] Larg MI, Barbus E, Gabora K, Pestean C, Cheptea M and Piciu D. 18F-FDG PET/CT in differentiated thyroid carcinoma. Acta Endocrinol (Buchar) 2019; 15: 203-208.

[26] Fonti R, Conson M and Del Vecchio S. PET/CT in radiation oncology. Semin Oncol 2019; 46: 202-209.

[27] Wang TA, Xian SL, Guo XY, Zhang XD and Lu YF. Combined 18F-FDG PET/CT imaging and a gastric orthotopic xenograft model in nude mice are used to evaluate the efficacy of glycolysis-targeted therapy. Oncol Rep 2018; 39: 271-279.

[28] Zhao C, Chen Z, Ye X, Zhang Y, Zhan H, Aburano T, Tian M and Zhang H. Imaging a pancreatic carcinoma xenograft model with 11C-acetate: a comparison study with 18F-FDG. Nucl Med Commun 2009; 30: 971-977.

Supplementary Video 1. Surgical procedure of the novel simple suture method.

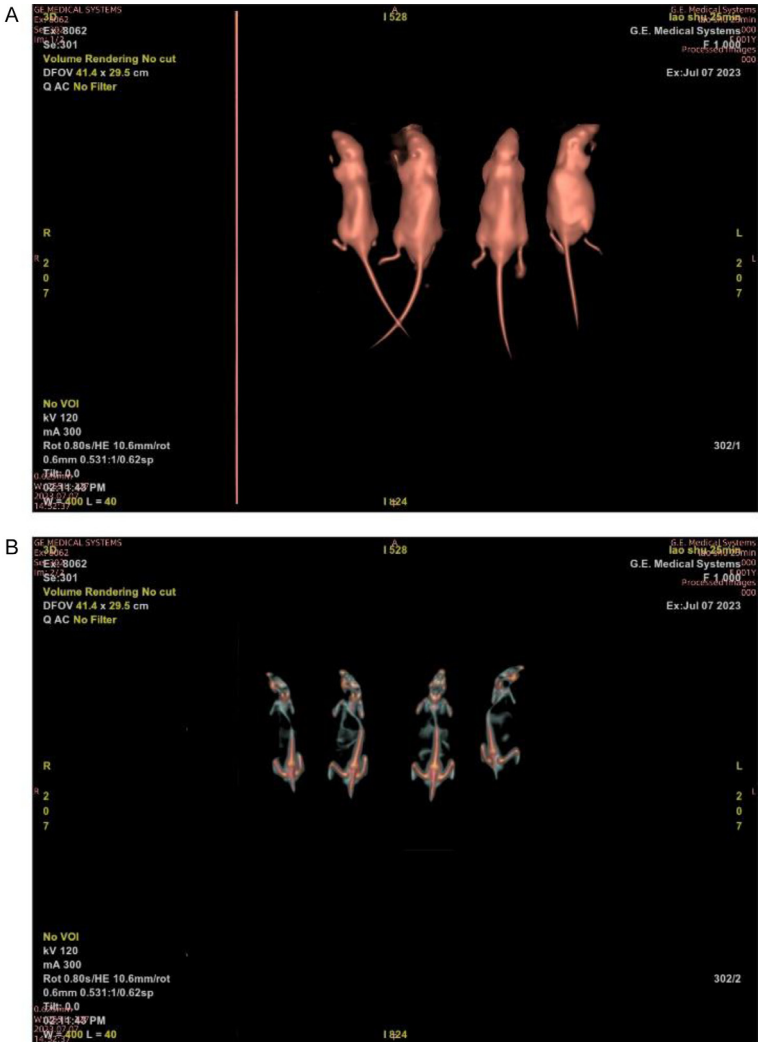

Supplementary Figure 1. PET/CT images. A, B. Three-dimensional (3D) reconstruction images.